Numerical Investigation of Flow Unsteadiness and Heat Transfer on Suction Surface of Rotating Airfoils within a Gas Turbine Cascade

Liang Guo[a,b], Yuying Yan[b]* , Wanchen Sun[a]*, Jie Zhu[b]

a. State Key Laboratory of Automotive Simulation and Control, Jilin University, Changchun 130022, China

b. Fluids & Thermal Engineering Research Group, Faulty of Engineering, University of Nottingham, Nottingham NG7 2RD, UK

Abstract: The effects of the periodical turbulence and pressure fluctuation on suction surface heat transfer over airfoils of a row of rotor blades with a certain type have been investigated numerically in this paper. The calculation is performed using $\overline{v^2}-f$ model with the numerical results of pressure fluctuation and heat transfer performance over 4 sample points being analyzed and compared with existing experimental data. It shows that the static pressure change has significant impact on heat transfer performance of the fore suction surface, especially in the active region of the shock waves formed from the trailing edge of upstream nuzzles. While, for the rear suction surface, the flow turbulence contributes more to the heat transfer change over the surface, due to the reduced pressure oscillation through this region. Phase shifted phenomenon across the surface can be observed for both pressure and heat transfer parameters, which should be a result of turbulence migration and wake passing across the airfoil.

Keywords: gas turbine cascade; Water ramjet; flow unsteadiness; pressure fluctuation; heat transfer; blade suction surface;

Nomenclature

C_r	chord length of rotor blade
C_μ	coefficient for $k-\varepsilon$ model
f	elliptic relaxation function of $\overline{v^2}-f$
Nu	Nusselt number
P	pressure
$\dot{q}$	heat flux
Re	Reynolds number
T	temperature
Tu	turbulence intensity
x,y	x and y coordinate
k	turbulence kinetic energy

Greek letters

ε	dissipation rate of turbulence kinetic energy
κ	thermal conductivity
ρ	density
μ_t	eddy viscosity
μ′	fluctuating velocity
$\overline{v^2}$	scalar velocity scale

Subscripts

1	inlet of nozzle guide vane
2	exit of nozzle guide vane
3	exit of rotor blade
s	static
t	total
gas	parameter relates to freestream condition
wall	parameter relates to wall condition
x	in x direction
y	in y direction

1. Introduction

*Corresponding author: Tel.: (44)115 95 13168. E-mail address: yuying.yan@nottingham.ac.uk, sunwc@jlu.edu.cn

The fluid flow across the turbomachinery has extremely high unsteadiness which is influential to the whole turbine system. It has been proved that the performance of heat transfer upon the engine components can be affected significantly by the turbulent flow and also the turbulence induced boundary layer transition. In order to further increase the thermal efficiency with an extended lifetime of the modern turbine engine, an in-depth understanding on the behaviors of the unsteady flow through the turbine cascade is therefore very important.

Over the past decades, many studies have been carried out to investigate the essence of flow turbulence and its effect on the boundary layer transition. The theoretical system about the turbulent flow and laminar-to-turbulent transition were built up gradually [1-4] with the mechanism of the transition becoming more clear. For the gas turbine, the effect of the free stream turbulence on turbine component heat transfer is a key factor that determines the thermal efficiency of turbomachinery [5-8]. A large amount of experimental studies have been carried out to investigate the effect of flow unsteadiness on boundary layer separation and surface heat transfer of turbine blades. Rhee et al. [9] reported that the blade relative position changes the incoming flow significantly which leads to variations in velocity and turbulence intensity of the cascade flow. With the changing relative position, the maximum difference in heat/mass transfer coefficients in certain region could be 30–50% of the average value. According to experimental results of Schobeiri et al. [10, 11], velocity behaviour was completely decoupled from thermal boundary layer but the thermal behaviour is tightly coupled with the boundary layer aerodynamics. In addition, increasing the turbulence level of the cascade flow mitigates the boundary layer transition, and the effects of the unsteady wake on time-averaged heat transfer coefficient can retain noticeable until the wakes are completely merged into the freestream turbulence. The effects of turbulence and unsteady wake entrained by a coming flow on convective heat transfer of a heated cylindrical surface were experimentally studied by Huang et al. [12]. They concluded that the upstream wake does not only produce stronger turbulence downstream, but also causes enhanced heat transfer upon the corresponding surface. Although, it is hard to deny that the experimental methods can bring most truthful results, but it is still difficult to carry out any transition related experiments under real engine operating circumstances, due to large difference between the environments of laboratory and engine cascade, conflicting conclusions may be obtained from similar objective reality. Thus, for experimental studies, a thorough understanding into the mechanism of the influence of turbulent flow on surface heat transfer can only be expected when more sophisticated technology is available.

As an alternative of confined experimental methods, the numerical approaches are wildly applied to provide addition solutions for the turbulence-heat transfer problems. Benefited from the rapid development of modern computing technology, the computational researches with higher accuracy and more reliability become accessible. Direct numerical simulations of flow and heat transfer in a turbine cascade with incoming wakes were carried out by Wissink and Rodi [13-15], the impinging induced flow structure changes are depicted in their studies and it shows that along the pre-transitional region of the suction surface the calculated heat transfer can be significantly increased by the free stream fluctuations, and this is regarded as a resulted of the introduced streamwise vortices into the boundary layer. Choi et al. [16] explained the mechanism of the turbulence enhanced heat transfer. The increasing turbulence intensity triggers earlier boundary layer transition and promotes a broader transition region. And then it disturbs the separated laminar boundaries and will finally result in spread of the enhanced heat transfer in relevant region. Guo et al.[17][18] studied the effects of turbulence on performance of cooling flow applied to gas turbine blade, it shows that the less the turbulence, the higher the film cooling effectiveness and lower heat transfer between mainstream and blade walls. Hwang et al. [19] conducted an analysis for steady-state and unsteady-state conjugate heat transfer for an aeronautic high pressure gas turbine, the calculation results shows that due to nozzle exit flow, the blade surface experiences relatively cooler and hotter temperature fields periodically, with a maximum temperature difference of around 450 K at the leading edge of blade being achieved. Similarly, investigations carried out by Schmidt et al. [20] and Chung et al. [21] show that any variations in the flow field, such as vortex migration and boundary layer transition will lead to direct change in heat transfer coefficient of different levels between mainstream gas and blade walls.

Although different studies has revealed the impacts of pressure fluctuation and flow turbulence on blade heat

transfer from different point of view; the coupling effects of the above two flow parameters at various blade locations are still not so clear at the current stage. Due to the extremely complicated flow condition within the cascade and high speed rotation of the blade during operation, the role of each contributing factors might vary with the engine turning. For further increase of engine efficiency and extension of components' lifetime, the coupling effects of these unsteady factors must be complete understood. In order to identify the independent influence of different contributing factors to the suction surface heat transfer, an integrated investigation is carried out numerically in the present work focusing on transient effects of different factors, especially, the specific role of mainstream turbulence and pressure fluctuation on surface heat transfer at different locations upon the aerofoil.

2. Problem definition:

A 2-dimensional physical model has been previously built up based on a real geometry from existing turbine system [22] with all boundary conditions being set in accordance with existing reliable experiments. Detailed information of the physical model and numerical procedure are presented below.

Geometry and boundary condition

The blade geometry is firstly extracted from a 3-D geometry with a curve-fitted sheet at 50% blade height and then projected onto an orthogonal plane. As shown in Fig.1, the full domain of the turbine cascade consists of 3 nozzle guide vanes and 5 rotor blades, pressure controlled inlet and outlet conditions are adopted for the modeling work.

A sliding interface condition is applied for the stage interface between the nozzle guide vanes and the rotor blades. No slip boundary conditions are used for all blades' wall with a constant wall temperature, while, for the top and bottom boundaries along each cascade in streamwise direction are enforced as periodical.

More detailed information of cascade parameter and flow configurations are given in Table.1.

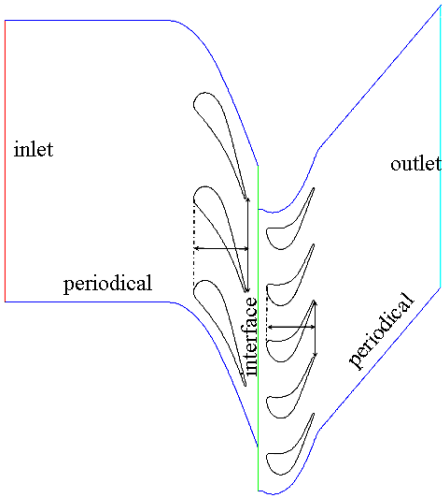

Figure 1 Computational domain and boundary conditions

Table 1 cascade parameter and flow configurations

Vane Cx (mm)	24.4
Blade Cx (mm)	21.78
Vane Pitch (mm)	42.8
Blade Pitch (mm)	26
Vane stagger angle (deg)	—
Blade stagger angle (deg)	—
T_1 (K)	393
P_{t1}/P_{s3}	4.02
Tu_1 %	1
Rotation frequency (1/s)	9300

Grid Generation

In the present study, a qualified grid system is constructed with body-fitted multi-block quadrilateral mesh, as shown in Fig. 2. The grids lines are generated nearly orthogonal to the boundaries; mesh check shows that no considerable discontinuity could be tracked. Two parts of the domain (part 1, nozzles and part 2, rotors) are initially built unattached and then combined at the stage interface during the grids post-processing. The nodes for different parts are specified as, streamwise 181× interface 222 for part 1, and streamwise 266× interface 247 for part 2, respectively. Grids are particularly fined for the critical regions close to the leading and trailing edges of all blades. A grid independent study was performed using doubled grids for all boundary layers with grids in other region being increased correspondingly. The grid independent study was achieved using the $\overline{v^2}-f$ model ran a general flow condition. The isentropic Mach number

distribution on nozzle surface was used as the criterion for independent examination. It shows that for the present grid scheme and the refined one, the difference of averaged isentropic Mach number on pressure surface was less than 0.05%, while this difference for the suction surface was no more than 0.12%. Considering the computational cost and the result accuracy, the current grid configuration was therefore selected as the suitable scheme for the modeling work. The grids were further adapted and refined using the mesh refinement function provided by the software during the simulation process, the gradient of the flow Mach number is used for a refinement criterion. Hereinto, the y^+ values in the study have be examined to be no more than 1.6 for the leading and trail edges of all blades and being no more than 3.5 for any other walls.

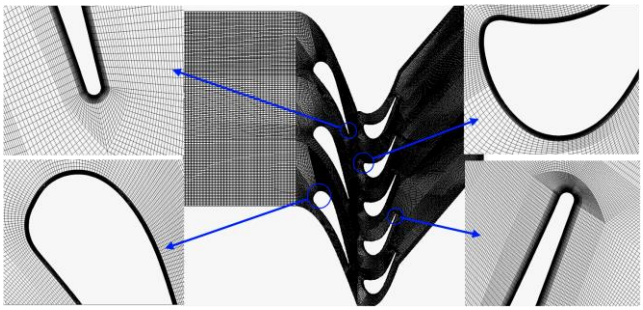

Figure 2 Grid scheme with a zoomed view of leading and trailing edge mesh

Solver and turbulence closure

Compressible ideal gas law is applied to the present simulation with the constant pressure, specific heat C_p, dynamic viscosity μ and thermal conductivity κ being expressed as piecewise polynomial functions of the static temperature [27]. A density based implicit solver is chosen for solving the governing equation system. The conservation equations is considered converged when the normalized residual of the energy equation is lower than 10^{-6} while the normalized residuals of continuity and other variables are less than 10^{-3}.

According to our previous investigation [22] and existing literatures [23-25] relating to aerodynamic and heat transfer modeling of cascade flow, the $\overline{v^2}-f$ model has been confirmed more capable in giving realistic and physical predictions for the transient rotation process, comparing to normal linear RANS models. Especially, for phenomenon such as transition induced heat transfer fluctuation and wake shedding process in regions near the walls, the $\overline{v^2}-f$ model provides better scaling of the damping of turbulent transport, thus, it was selected for present study.

Here, the $\overline{v^2}-f$ model by Durbin [26] belongs to nonlinear eddy viscosity models that is similar to the Standard k-ε model. Instead of turbulent kinetic energy k, it uses a velocity scale $\overline{v^2}$ for the evaluation of the eddy viscosity, and therefore, the equations for k and ε are supplemented by the equation for $\overline{v^2}$,

$$\partial_t(\rho\overline{v^2})+\nabla\cdot(\rho\rho\,\overline{v^2})=\rho kf-\rho N\frac{\overline{v^2}}{k}\varepsilon+\nabla\cdot((\mu+\mu_t)\nabla\overline{v^2}) \quad (1)$$

The turbulent viscosity in $\overline{v^2}-f$ model is defined as:

$$\mu_t=C_\mu\rho\overline{v^2}T \quad (2)$$

where $\overline{v^2}$ can be regarded as the velocity fluctuation normal to the streamlines; and T, the turbulence time scale, is defined as:

$$T=\min\left[\max\left[\frac{k}{\varepsilon},6\sqrt{\frac{\nu}{\varepsilon}}\right],\frac{\alpha k}{\sqrt{6}\overline{v^2}C_\mu|S|}\right] \quad (3)$$

3. Results and Discussions

As mentioned in previous chapter, to understand the effects of the upstream unsteady flow on aerodynamic and heat transfer performance of the blade, relevant parameters, including pressure fluctuation and Nu number from four points along the suction surface of one rotor blade were examined. The detailed coordinate of each point along the X direction can be found in Table 2, and a distribution of the sample points along the wall is given in Fig. 3.

Table 2 Sample point coordinates

Sample Point	Normalized C_{rx}
Min	0.0
141	0.0367
139	0.1820
140	0.5120
138	0.6130
Max	1.0

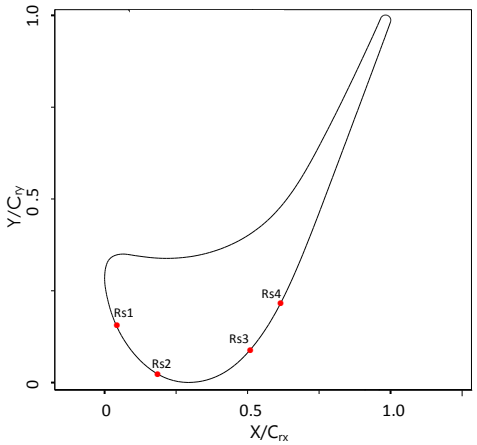

Figure 3 Distribution of the sample points along the blade suction surface

Pressure fluctuation along the suction surface

Flow unsteadiness along the suction surface of the aerofoil in this study is predicted with the pressure fluctuation upon four sampling points. The results are then compared with reliable experimental data measured from a turbine cascade of a same structure of reference[22]. In order to eliminate the random error of the measurement and calculation, all pressure data presented here is ensemble averaged during the post processing. History of the rotor movement is expressed in fractions of the blade passing events. Pressure fluctuations over the four sample points in 3 blade passing periods are shown in Fig. 4. Note the fluctuations are not depicted with any absolute value of total/static pressure, but the differences between the mean total pressure across the rotor inlet and the time dependant stagnation pressure calculated for each sampling point. By this way, the pressure fluctuation would be highly sensitive to any tiny unsteadiness that occurred at different flow time. In addition, the flow times for the occurrence of shock wave and unsteady wake against the blade moving fraction are marked out with the dash-dotted lines I and II, respectively, as seen in Fig.4.

For the amplitude of pressure fluctuations, it can be concluded that the value over points Rs1 and Rs2 are much higher than that over the other two points, Rs3 and Rs4. In consideration of the locations of the sample points, it reveals that the comparing to the effects of the mainstream flow, the blade-interaction exerts much more influences to pressure field change around the rotor blade, especially for the fore suction surface close to the leading edge. As seen in Fig.4, when the sampling point Rs1 approaches the shock wave of which the location is marked out by line Ⅰ, a series of quick oscillations could be found along the measured pressure curve before the marker line, following by a quick boost in pressure upon the Rs1. This should be caused by the significant changes in pressure field around the leading edge wall of the rotor, as a result of shock wave attack at this flow time. A similar pressure change could also be seen for sample point Rs2, however due to the rearward position of Rs2; the pressure changes upon it come a bit late comparing to that upon point Rs1.

For the sample points located on rear suction surface, the pressure undulation over Rs3 and Rs4 can be found much milder than those reported by Rs1 and Rs2. This indicates that the leeward position of sample points on rear suction surface restrains the effects of flow unsteadiness generated from the blade-interactions, which makes the rear suction surface to be less affected by incoming flow, and thus more uniform temperature field and more steady heat transfer characteristics. In addition, comparing to the fore part of the rotor, the rear suction surface is much closer to the stage exit, thus, amplitudes of pressure undulation degrade gradually with the location the sample point, the closer the location to the exit, the smaller the amplitudes of pressure changes.

For Fig. 4, magnitude of the calculated fluctuations on each sample point is seen smaller than the test results, especially for Rs1 and Rs2. Possible reasons for differences between the predictions and the measurements can be roughly summarized as follows:

Firstly, the modeling is achieved using a 2-D scheme which should be considered as the most important source for any imperfect solution of the present simulation. Due to the absence of dimension along the blade thickness, the effects of the spanwise pressure gradient on flow behaviours are missing; and therefore, the radial velocity fields through the turbine cascade cannot be predicted correctly during the simulation. Lack of the above information in the third dimensionality will result in over-predicted Reynolds stresses throughout the domain, further, an over-predicted pressure field and under-predicted fluctuation level across the turbine stage [27].

Another influential factor for the differences between the numerical and experimental results, especially the pressure fluctuations with higher frequencies, is the change in flow incident angle owing to the shock wave structure or reflected shocks from the reality. Such changes could be caused by any

random turbulence occurred during the shock wave propagations which is unpredictable. The effects of these turbulent factors are much more dominant for point Rs1 and Rs2, due to the stronger interaction between the mainstream flow and the blade wall in the region close to the nose of rotor blades. This can also explain why a better agreement between the predicted results and the test data can be achieve for sample points Rs3 and Rs4 that are located much closer to the trailing edge, thus being less influenced by the upstream shock wave and the unsteady wake generated from upstream nozzles.

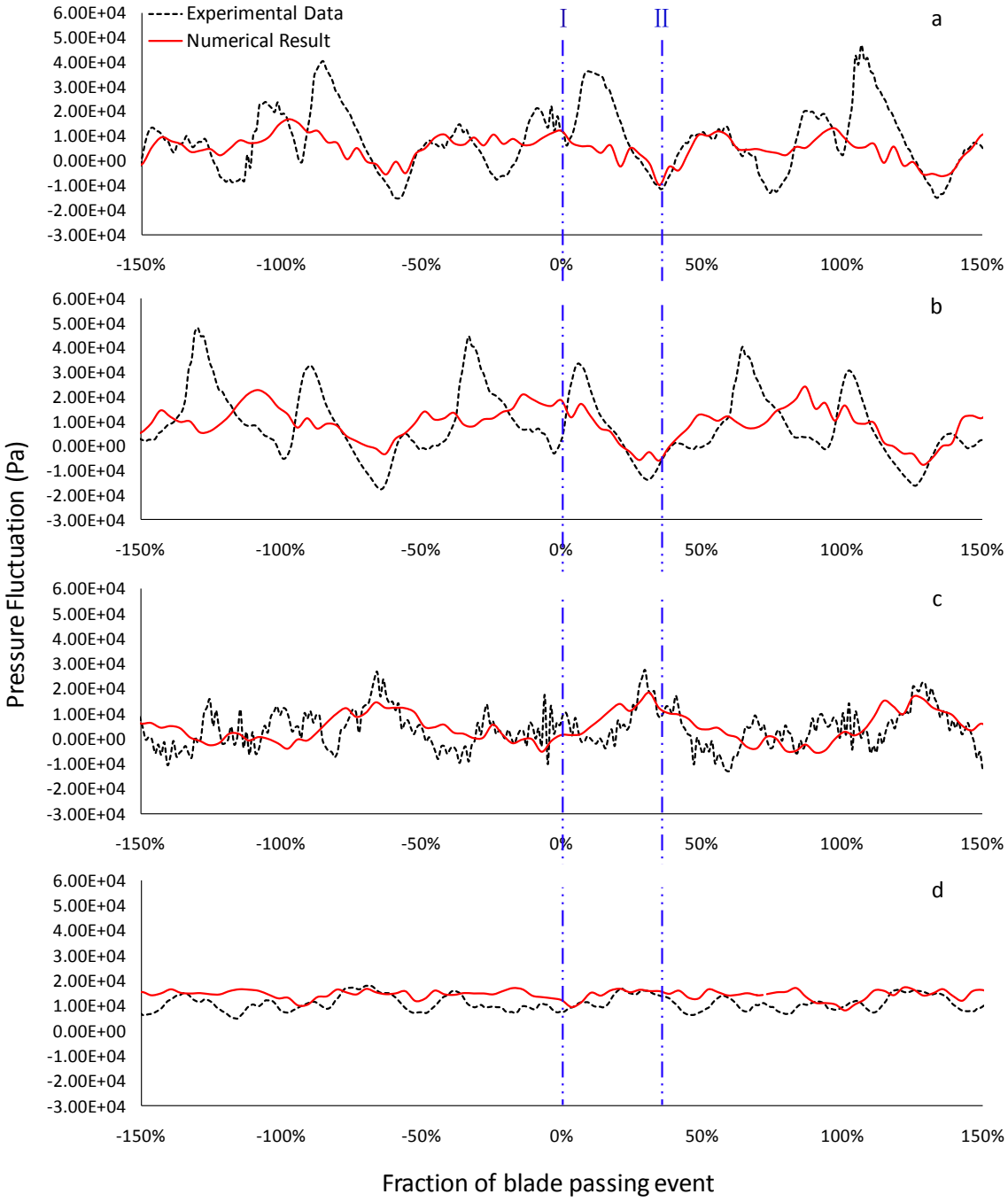

Figure 4 Comparison of the pressure fluctuation between the numerical data and ensemble averaged experimental result

a. Point Rs1 b. Point Rs2 c. Point Rs3 d. Point Rs4

In addition, as mention before, the fluctuations displayed here are depicted with the pressure differences between the mean total pressure and the time dependant stagnation pressure, which has been testified to be much more sensitive

to the flow unsteadiness. Although our previous study [22] shows that the code is capable in bringing accurate prediction of averaged static pressure distribution around the blade walls, but it seems that it is not capable in capturing all the detailed time dependant pressure oscillations caused by coupling effects of random turbulence and specific geometrical structure of the real blade cascade. However, considering the complicated flow conditions and sharp pressure gradient throughout the turbine cascade, the results are deemed in an acceptable range for understanding the target objective of the present study.

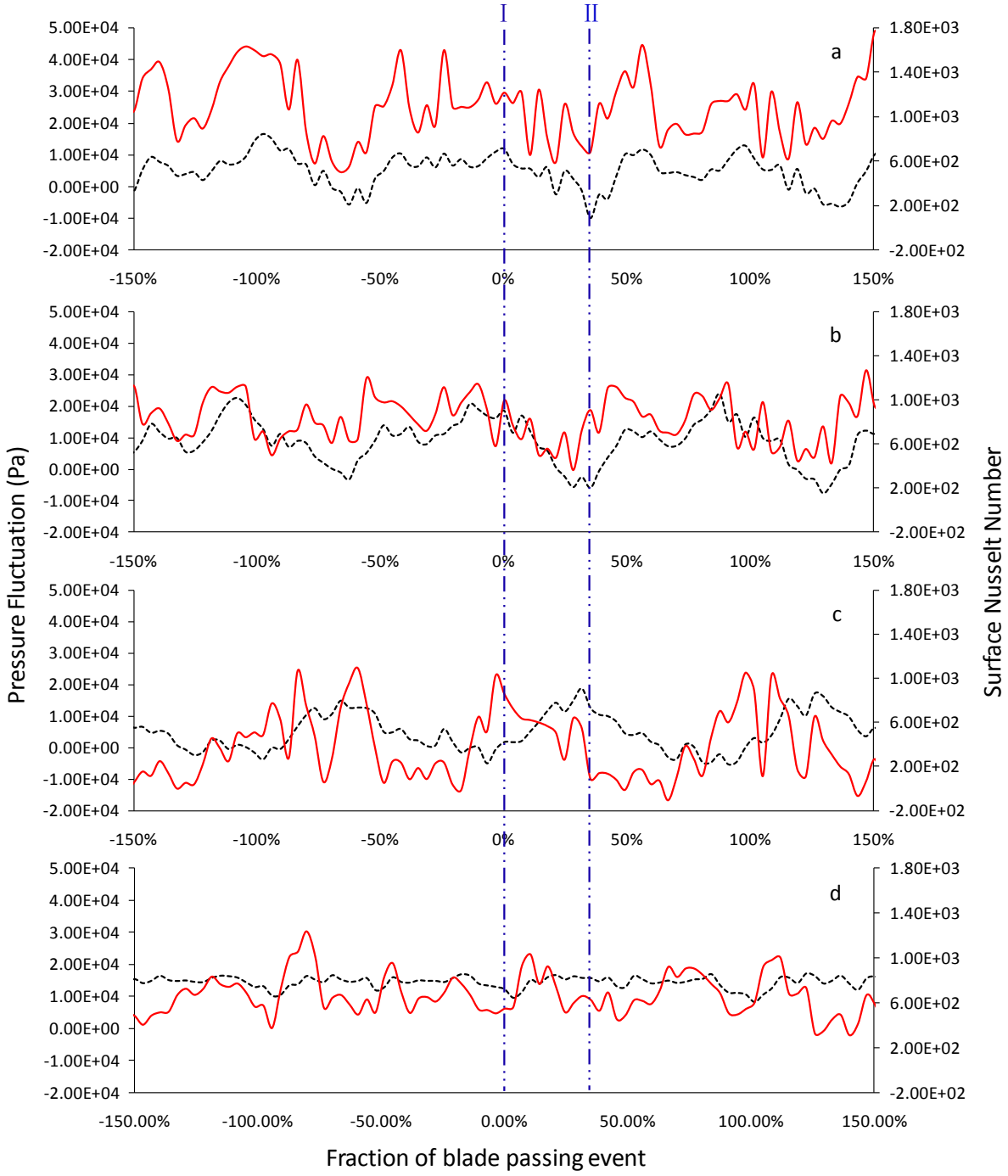

Figure 5 Comparison of the surface Nu number fluctuation between the numerical data and ensemble averaged experimental results a. Point Rs1 b. Point Rs2 c. Point Rs3 d. Point Rs4

Surface heat transfer

Predicted Nusselt number (*Nu*) over each sample point in three blade passing periods is presented in Fig. 5. The results are analyzed in contrast with the calculated pressure fluctuation shown in Fig. 4. In this study, the Nusselt number is defined by the following equation,

$$Nu = \frac{\dot{q}L}{(T_{gas} - T_{wall})\kappa} \quad (4)$$

where $\dot{q}$ is the heat flux through the blade wall, κ is the thermal conductivity of the air which is evaluated as discussed in section 2.3, the chord of the rotor blade C_r is used as the length-scale *L*, T_{gas} and T_{wall} are the cascade inlet total temperature and the calculated local wall temperature reported by each grid node around the aerofoil.

For the magnitude of heat transfer, the highest *Nu* shown in Fig.5 is given by point R_{s1} which is situated in the vicinity of the leading edge. The second highest *Nu* is from R_{s2}, the sample point also situated upon the fore suction surface. Sample points R_{s3} and R_{s4} give the lowest *Nu* values among the four, with both of them being located in the rear suction surface. Considering the entire history of the surface heat transfer at different locations, it indicates that the fore part of the suction surface bears a higher heat flux than the rear part. Comparison between each sub-charts of Fig.5 also shows that the *Nu* reduces all the way along the blade chord towards the trailing edge. As analyzed in last section, the fore part of the airfoil is exposed to the region with the highest pressure fluctuation; it therefore results in a high turbulent boundary layer over the surface, thus higher convection between the gas and the blade walls.

For the heat transfer fluctuation, Rs1 presents more significant changes than Rs2 in the fore region of the suction surface, while; Rs3 brings bigger amplitude of fluctuation than R_{s4} in the rear region. It can be found that the fluctuation of the local Nusselt number is coincident with the pressure oscillation to a certain extent. The relationship between local heat transfer and pressure parameters indicates that penetrating effect upon the boundary layer derived from the pressure fluctuation is one important source for heat transfer variation over the surface. Due to the its unfavorable location, the fore suction surface of the blades bears brunt of the pressure undulation caused by upstream shock wave and unsteady wakes, and therefore, higher burden of heat transfer between the mainstream flow and blade surface.

Instantaneous Turbulence pattern

In order to understand more about the mechanism of impact of instantaneous flow structures on local surface heat transfer over the examined surface, the flow structures at different flow time in the vicinities of each sample point were examined and depicted with intensity of turbulence kinetic energy (TKE) , as shown in Fig. 6 and Fig. 7.

Fore part of the airfoil

Fig. 6(a) presents the instantaneous flow structure near the fore suction wall at 0% blade passing fraction. Referring to Fig. 4, it knows that at this flow time, the rotor blade is approaching the shock region downstream of the corresponding nozzle. As seen from Fig. 6 (a), the flow turbulence level near the sample points Rs1 and Rs2 is much higher than that depicted in other sub-charts of Fig. 6. The turbulence distribution along the blade wall also becomes extremely uneven which can be reflected by the history of *Nu* shown in Fig. 5, clearly, at the 0% blade passing fraction, the *Nu* over R_{s1} and R_{s2} becomes more volatile comparing to other flow time. However, comparing to point $R_{s1,}$ the *Nu* over R_{s2} goes down much quicker with the shock passing, illustrates that the local impacts of shock wave exerted to airfoil varies with location upon the surface.

Instantaneous flow structures at 25% blade passing fraction are depicted by Fig.6(b). Referring to Fig. 4, at this flow time, the leading edge of the rotor nearly arrives the onset of unsteady wake. The vortex structure in front of the blade wall, upstream, from -0.25 to -0.1 of X/C_{rx} indicates the exact location of the incoming wake. Although the turbulence intensity of the flow in the wake region is high, the flow field adjacent to the blade wall is found much more organized with only milder turbulence gradients distributing along the suction surface. The pressure measurement result shown in Fig.4 indicates right after the current flow time, the fore part of the blade will migrates into a low pressure zone derived from the wake passing. The pressure fluctuation (shown in Fig.4) and flow turbulence (shown in Fig. 6) near the fore suction wall could be both reduced temporarily. As a result, reductions in the local heat transfer coefficients upon R_{s1} and R_{s2} could be observed in Fig. 5.

As shown by Fig. 6, at the flow time of 55% blade passing, the magnitude of the flow turbulence adjacent to the leading edge is found increasing regularly with the blade travel, but

the turbulence field is seen remaining organized. The turbulence field around the rotor is mainly determined by the pressure filed of the same region. On one hand, the blade arrives a medium-high pressure zone caused by the interaction between the rotor and the approaching vane for the next blade passing event. With the migration of the tracked rotor, the flow passageway between the rotor and the incoming vane shrinks at the current flow times. And the narrowed spacing further leads to an increased pressure over the sample points. On the other hand, the adhesive force between the gas and the wall is strengthened by the increased static pressure upon the surface which prevents the flow from being more turbulent. To accompany the pressure rise and turbulence reduction, the total temperature in the vicinity of the wall increases correspondingly strengthening the surface heat transfer of the fore suction surface. According to the above analysis, it can be concluded that the heat transfer enhancement on R_{s1} and R_{s2}, at this flow time, should be a result contributed jointly by the pressure rise and turbulence increment of the flow.

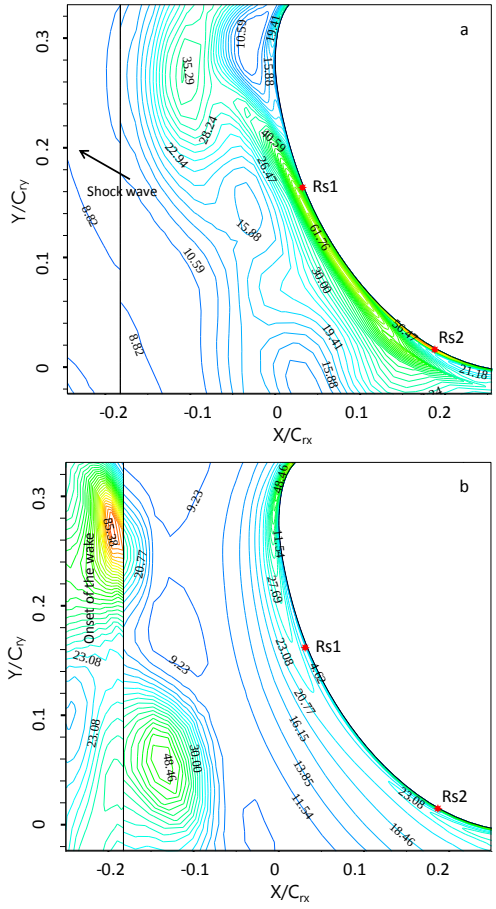

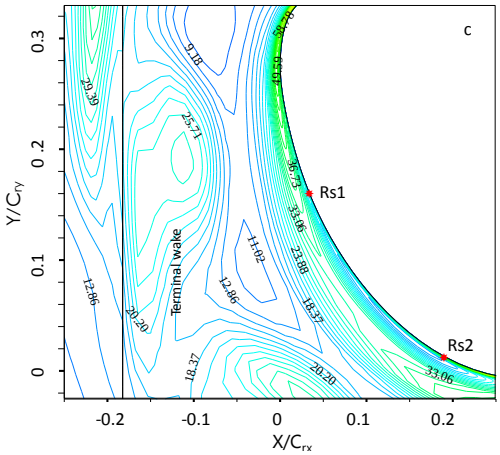

Figure 6 Instantaneous flow structure in the near wall region (Fore part of the airfoil)

(a) 0% blade passing (b) 25% blade passing (c) 55% blade passing

Rear part of the airfoil

Fig. 7 presents a closer view of the flow structures round rear part of the rotor blade (X/C_{rx}=0.3~X/C_{rx}=0.8). Three different blade passing fraction of 45%, 75% and 10% are chosen as typical flow time for demonstrating the role of different flow structures. Compared to the flow turbulence near the fore suction surface, the turbulence level near the rear suction side is relatively high. It has been proved by both experimental and numerical results that the pressure fluctuation in this region is low. Thus, migration of the incoming wake is thought to be the major contributing factor to the high turbulence in this region.

Fig. 7(a) shows that at the 45% blade passing fraction, the turbulence in both near wall region and the mainstream region is at a lower level. This is because that at this flow time, the lower segment of the chopped wake has not yet reached the rear part of the blade. As a direct result of the weak turbulence field, lower *Nu* are reported by R_{s3} and R_{s4}, respectively, as it is shown in Fig. 5.

With the blade movement, at 75% blade passing fraction, the fore part of the aerofoil has nearly cut through the wake flow. And the wake induced unsteadiness has passed through the crown region reaching to the rear suction surface. This can be reflected by the high turbulence level near the blade wall as shown in Fig.7(b). Compared with Fig.7(a), at 75% blade passing fraction， the gradients of flow turbulence in free stream is found strengthened. Along the suction surface, the peak value of TKE occurs near R_{s4}. Because at this flow

time the pressure oscillations over R_{s3} and R_{s4} are considerably low (see Fig. 4), thus the strengthened flow turbulence rather than the pressure fluctuation is thought to be the dominant factor for the promoted *Nu* upon the rear wall.

Fig. 7(c) displays the flow structure at 10% flow time. With the development of the wake flow, the unsteadiness goes further towards the trailing edge of the rotor blade. Accordingly, a reduced TKE value can be observed at sample point R_{s3}.While, a sharp rise in the flow TKE value are found for the region round R_{s4}. Referring to Fig. 5 (d), although the *Nu* over Rs3 remains a high level, it tends to decrease as a result of the gradually weakened turbulence attributed to the receding wake. At the same flow time, Nu over Rs4 reaches the peak due to the rapidly increased turbulence above the boundary layer.

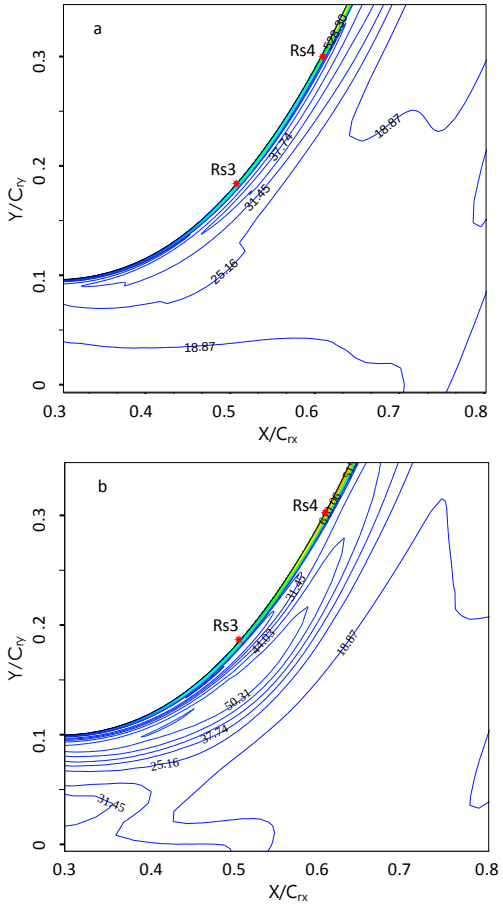

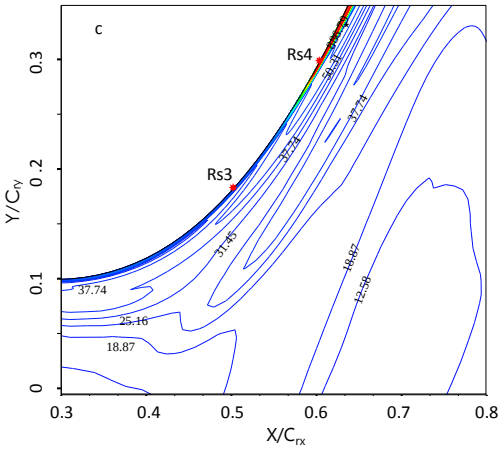

Figure 7 Instantaneous flow structure in the near wall region (Rear part of the airfoil)

(a) 45% blade passing (b) 75% blade passing (c) 10% blade passing

In addition, it can be seen that the magnitude of TKE over Rs4 at 10% blade passing exceeds the values of Rs1 and Rs2, but the Nu reported by Rs1 and Rs2 are still much higher than that of Rs4. This comparison illustrates that although the wake migration induced turbulence could result in fluctuations in heat transfer along the wall, but it is not significant enough to dictate the degree of heat transfer rate upon the surface

4. Conclusion

The static pressure fluctuations, flow turbulence and the history of Nu over the suction surface of a tracked rotor blade are numerically calculated, analyzed and reported in this work. Obtained with the $\overline{v^2}-f$ model, the numerical results show reasonable agreements with the experimental data in frequency of the pressure undulation. Sources of the deficiencies in predicting amplitude of the pressure fluctuation are found to be introduced mainly by of 2-D scheme applied for the modeling work. Such deficiency can be expected eliminated with a 3-D modeling scheme in future work.

For the fore suction surface, the heat transfer performance of the blade are significantly influenced by the time-varying pressure filed in the vicinity of wall, as the variation of Nu on the surface is found being consistent with the pressure undulation to a certain degree. The blade-interaction induced pressure fluctuation is the dominant source for changes of the

temperature field. Although the wake and other factors induced flow unsteadiness also plays an important role in affecting the heat transfer distribution upon the surface, less impacts from the unsteadiness can be taken into account when it compares to that of the pressure field.

For the rear part of the suction surface, due to the degraded effect of the mainstream pressure, the influence of the flow turbulence on heat transfer becomes more effective; a higher level of boundary layer turbulence leads to higher amplitude of heat transfer fluctuation, however, this effect is still not that significant to dictate the degree of heat transfer rate upon the surface.

Acknowledgement

The authors gratefully acknowledge the financial support from China Scholarship Council (CSC) and Siemens Industrial Turbomachinery Ltd. (UK) for Liang Guo's PhD research at the University of Nottingham Nottingham (RIS 101798).

Reference

[1]Walker, G.J. and J.P. Gostelow, Effects of adverse pressure gradients on the nature and length of boundary layer transition. Journal of Turbomachinery, 1990. 112: p. 169-205.

[2]Mayle, R.E. and K. Dullenkopi, A theory for wake-induced transition. Journal of Turbomachinery, 1990. 122: p. 189-195.

[3]Walker, Q.J., The role of laminar-turbulent transition in gas turbine engines: a discussion. Journal of Turbomachinery, 1993. 115: p. 207-216.

[4]Dring, R.P., Boundary Layer Transition and Separation on a Compressor Rotor Airfoil. Journal of Engineering for Power 1982. 104(1): p. 251-253.

[5]L Guo, YY Yan, JD Maltson, Numerical study on discharge coefficients of a jet in crossflow, Computers & Fluids 49(1) (2011), 323-332.

[6]YQ Zu, YY Yan, J Maltson, Numerical study on stagnation point heat transfer by jet impingement in a confined narrow gap, Journal of Heat Transfer 131 (9) (2009), 094504.

[7]S Huang, JD Maltson, YY Yan, Experimental study on heat transfer improvement structures with staggered transverse elongated pedestal array, International Journal of Heat and Mass Transfer 97 (2015), 502-510.

[8] Song L, Zhu P, Li J, et al. Effect of Purge Flow on Endwall Flow and Heat Transfer Characteristics of a Gas Turbine Blade[J]. Applied Thermal Engineering, 2016, 110:504-520.

[9]Rhee, D.-H. and H.H. Cho, Effect of vane/blade relative position on heat transfer characteristics in a stationary turbine blade: Part 2. Blade surface. International Journal of Thermal Sciences, 2008. 47(11): p. 1544-1554.

[10]Schobeiri, M., K. Read, and J. Lewalle, Effect of unsteady wake passing frequency on boundary layer transition, experimental investigation, and wavelet analysis. Journal of Fluids Engineering, 2003. 125(2): p. 251-266.

[11]Schobeiri, M., et al., On the physics of heat transfer and aerodynamic behavior of separated flow along a highly loaded low pressure turbine blade under periodic unsteady wake flow and varying of turbulence intensity. Journal of heat transfer, 2008. 130(5): p. 051703.

[12]Huang, C., Y. Cheng, and Y. Kang, Combined effect of grid turbulence and unsteady wake on convective heat transfer around a heated cylinder. International Communications in Heat and Mass Transfer, 2007. 34(9): p. 1091-1100.

[13]Wissink, J. and W. Rodi, Direct numerical simulation of flow and heat transfer in a turbine cascade with incoming wakes. Journal of Fluid Mechanics 2006. 569: p. 209-247

[14]Wissink, J.G., DNS of separating, low Reynolds number flow in a turbine cascade with incoming wakes. International Journal of Heat and Fluid Flow, 2003. 24(4): p. 626-635.

[15]Wissink, J. and W. Rodi, Direct numerical simulations of transitional flow in turbomachinery. Journal of Turbomachinery, 2006. 128: p. 668-678.

[16]Choi, J., et al., Effect of free-stream turbulence on turbine blade heat transfer and pressure coefficients in low

Reynolds number flows. International Journal of Heat and Mass Transfer, 2004. 47(14): p. 3441-3452.

[17]Guo L, Liu Z C, Yan Y Y, et al. Numerical Modeling and Analysis of Grooved Surface Applied to Film Cooling[J]. Journal of Bionic Engineering, 2011, 08(4):464-473.

[18]Guo L, Yan Y Y, Zu Y Q. Effect of Narrow Jet Spacing on Impinging Flow and Heat Transfer[J]. American Society of Mechanical Engineers, 2011.

[19]Hwang, S., et al., Comparative study on steady and unsteady conjugate heat transfer analysis of a high pressure turbine blade. Applied Thermal Engineering, 2016. 99: p. 765-775.

[20]Schmidt M, Starke C. Coupled heat-transfer simulations of turbines in consideration ofunsteady flows[J]. International Journal of Thermal Sciences, 2015, 96:305-318.

[21]Chung H, Hong C W, Kim S H, et al. Heat transfer measurement near endwall region of first stage gas turbine nozzle having platform misalignment at combustor-turbine interface[J]. International Communications in Heat & Mass Transfer, 2016, 78:101-111.

[22]Guo L., Yan Y., and Maltson J.D., Performance of 2D scheme and different models in predicting flow turbulence and heat transfer through a supersonic turbine nozzle cascade. International Journal of Heat & Mass Transfer, 2012. 55(s 23–24): p. 6757-6765.

[23]Manceau, R., S. Parneix, and D. Laurence, Turbulent heat transfer predictions using the V2F model on unstructured meshes. International Journal of Heat and Fluid Flow, 2000. 21(3): p. 320-328.

[24]Luo, J. and E.h. Razinsky, Conjugate heat transfer analysis of a cooled turbine vane suing the V2F turbulence model. Journal of Turbomachinery, 2007. 129: p. 773-781.

[25]Levchenya, A.M. and E.M. Smirnov. CFD-analysis of 3D flow structure and endwall heat transfer in a transonic turbine blade cascade: effects of grid refinement. in West-east high speed flow field conference. 2007. Moscow, Russia.

[26]Medic, G. and P.A. Durbin, Toward Improved Prediction of Heat Transfer on Turbine Blades. Journal of Turbomachinery, 2002. 124: p. 187-192.

[27]Mittal, R. and S. Balachandar, Effect of three dimensionality on the lift and drag of nominally two dimensional cylinders. Physics of Fluids, 1995. 7(8): p. 1841-1865